Chemoarchitectural Signatures of Subcortical Shape Alterations in Generalized Epilepsy

Wei Liao (weiliao.wl@gmail.com)
University of Electronic Science and Technology of China https://orcid.org/0000-0001-7406-7193
Yao Meng
Jinming Xiao
University of Electronic Science and Technology of China
Siqi Yang
University of Electronic Science and Technology of China https://orcid.org/0009-0008-4751-1664
Jiao Li
MOE Key Laboratory for Neuroinformation, University of Electronic Science and Technology of China
Qiang Xu
Jinling hospital https://orcid.org/0000-0002-7739-7515
Qirui Zhang
Jinling Hospital, Nanjing University School of Medicine https://orcid.org/0000-0002-3520-9336
Guangming Lu
Nanjing University https://orcid.org/0000-0003-4913-2314
Huafu Chen
University of Electronic Science and Technology of China
Zhiqiang Zhang
Lab. of Neuroimaging, Dept. of Radiology, Jinling Hospital, Nanjing University School of Medicine
https://orcid.org/0000-0002-3993-7330

Article

Keywords:

Posted Date: February 5th, 2024

DOI: https://doi.org/10.21203/rs.3.rs-3833408/v1

Additional Declarations: There is **NO** Competing Interest.

Abstract

Genetic generalized epilepsies (GGE) exhibit widespread morphometric alterations in the subcortical structures. Subcortical nuclei are essential for understanding GGE pathophysiology, but their fine-grained morphological diversity has yet to be comprehensively investigated. Furthermore, the relationships between macroscale morphological disturbances and microscale molecular chemoarchitectures are unclear. High resolution structural images were acquired from patients with GGE (n = 97) and sex- and age-matched healthy controls (HCs, n = 184). Individual measurements of surface shape features (thickness and surface area) of seven bilateral subcortical nuclei were quantified. The patients and HCs were then compared vertex-wise, and shape anomalies were co-located with brain neurotransmitter profiles. We found widespread morphological alterations in GGE and prominent disruptions in the thalamus, putamen, and hippocampus. Shape area dilations were observed in the bilateral ventral, medial, and right dorsal thalamus, as well as the bilateral lateral putamen. We found that the shape area deviation pattern was spatially correlated with norepinephrine transporter and nicotinic acetylcholine (Ach) receptor ($\alpha_4\beta_2$) profiles, but a distinct association was seen in the muscarinic Ach receptor (M_1).The findings provided a comprehensive picture of subcortical morphological disruptions in GGE, and further characterized the associated molecular mechanisms. This information may increase our understanding of the pathophysiology of GGE.

1. Introduction

Genetic generalized epilepsies (GGE) account for approximately 15%–20% of epilepsy patients[1,2]. GGE do not have apparent focal lesions, but exhibit widespread morphometric alterations across the cerebral cortex and subcortical structures[2–5]. Subcortical nuclei are essential for multiple cognitive and motor functions, and thus are hypothesized to play a central role in the neural circuitry pathology underlying GGE[6–8]. Numerous volumetric structural studies have determined the volume alterations of subcortical nuclei in GGE, but the results have been inconsistent, with both atrophy and expansion reported in the thalamus[9–12]. Volumetric analysis methods do not capture the shape complexities of subcortical structures, and therefore, are not well-suited for characterizing detailed morphological abnormalities that may be present in GGE[13]. Although subcortical nuclei are essential for understanding the pathological process in GGE, studies that comprehensively and systematically characterize morphological alterations of these structures remain scarce.

Surface-based approaches, such as the ENIGMA-Shape pipeline, provide an intuitive yet powerful means of quantifying anatomy. The pipeline reconstructs the boundary mesh of subcortical nuclei and generates vertex-wise morphological information. This approach detects more localized differences in brain structure, reveals subtle genetic and disease effects, and provides more relevant biological information when compared to aggregate descriptors such as volumetric measures[13–19]. High resolution surface-based shape analyses of subcortical structures have been used to characterize the genetic influence of morphometric variability[13], and sex and age effects over the lifespan of structural variations[20], and has

been used to map alterations in multiple brain diseases, including neurodegenerative diseases such as Alzheimer's disease[21,22], dementia[23], and psychiatric disorders such as major depressive disorders[24,25] and schizophrenia[26]. Shape analysis also provides the basis to bridge structural information with functional architecture[27], transcriptomic profile[28], and molecular chemoarchitecture. Thus, shape analysis of subcortical nuclei provides fine-grained morphometric information, revealing the distinctive influence of epileptic seizures on their subregions.

The imbalances of excitatory and inhibitory neurotransmitters have been thought to be a critical element contributing to the development of epileptic seizures[29]. Multiple neurotransmitters from different systems have been implicated in the pathogenesis of GGE[30]. The subcortical nuclei have close ties with neurotransmitter pathways and may be essential for the development of epilepsy[31]. The relationship between macroscale structural changes and microscale molecular neurotransmitter systems is poorly understood. Still, it may contribute to a better understanding of the association of cross-scale disease representation in the brain.

In this case-control study, we quantified morphological information regarding shape meshes of 14 subcortical nuclei. We systematically mapped alterations between genetic generalized epilepsy patients and healthy controls (HCs) in all subcortical structures. We then further investigated the associations between the morphological alteration levels and neurotransmitter expression profiles.

2. Results

2.1 Demographic information

This study included 97 patients diagnosed with GGE-GTCS (31 females, mean age = 25.44 ± 8.17 years) and 184 HCs (80 females, mean age = 25 ± 5.92 years). The age and sex were matched between the two groups (Table 1).

Table 1
Demographic and clinical characteristics of participants.

Demographics	HCs	GGE	Comparison
	(n = 184)	(n = 97)	GGE vs. HCs
Sex (female/male)	80/104	31/66	χ^2 = 3.53 (P = 0.06)
Handedness (left/right)	0/184	0/97	χ^2 = 0 (P = 1)
Age (years)	25 ± 5.92	25.44 ± 8.17	U = 7898 (P = 0.11)
Duration (months)	—	83.81 ± 93.32	—
Age at seizure onset (years)	—	18.46 ± 8.27	—

2.2 Subcortical surface-based morphology alterations

We used the ENIGMA-Shape pipeline to acquire the shape metrics of subcortical neculei (Fig. 1). Two surface vertex-wise morphological measures were defined: radial distance (RD) and Jacobian determinant (JD). The RD was the distance of each vertex to the medial curve, which was the core along the long axis of the structural skeleton. The RD was empirically considered to be a measure of shape “thickness”. The JD was the surface dilation ratio of mapping the corresponding vertices on individual-specific structure surfaces to the standard templates. The JD was a measure of shape “area”, and it resembled surface “contraction or expansion”.

We conducted vertex-wise group statistical comparisons between GGE patients and HCs. We observed extensive alterations of both surface-based morphological features, JD, or shape area and RD, or shape thickness in all subcortical structures in GGE (Fig. 2). However, only the thalamus and amygdala showed overall volume alterations in GGE (Suppl. Table 1). Patients exhibited dilations of shape surface areas (increased JD) in the bilateral ventral, lateral, and medial thalamus, dorsoanterior and ventroposterior putamen, dorsoanterior and tail caudate, and right hippocampus tail ($p < 0.05$, FWE corrected). However, they also exhibited contractions (decreased JD) in bilateral ventral nucleus accumbens, ventral amygdala, and dorsomedial caudate ($p < 0.05$, FWE corrected). The shape thickness profile showed that GGE were thicker (increased RD) in the anterior thalamus, lateral putamen, dorsal caudate, hippocampus head, and dorsal amygdala ($p < 0.05$, FWE corrected). However, they were also thinner (decreased RD) in the bilateral dorsoanterior and dorsoposterior caudate, ventral hippocampus, anterior amygdala, and ventral thalamus ($p < 0.05$, FWE corrected).

2.3 Subcortical neurotransmitter profiles

We collected 25 PET maps of 18 receptor/transporter corresponding to nine different neurotransmitter systems from the neuromaps toolbox[32]. These neurotransmitters included dopamine, norepinephrine, serotonin, acetylcholine, glutamate, GABA, histamine, cannabinoid, and opioid neurotransmitters. We then used the MSA atlas to parcellate these PET maps and projected each region in the volumetric atlas to a homologous region in the surface version atlas (Fig. 3A; Suppl. Figure 1). We visualized four maps associated with subcortical morphological alteration levels, which were explicitly explored in the following section. The first two maps involved PET maps from different sources. These maps indicated spatial distribution of the norepinephrine transporter (NET), which belongs to the norepinephrine (NE) transmitter system. The distribution pattern of NET was similar between the two maps, showing high concentration in the ventral and lateral of the bilateral thalamus, with the lowest expression in the caudate (Fig. 3B). The PET map that targeted α4β2, a receptor in the nicotinic acetylcholine neurotransmitter system, indicated a high concentration in the thalamus, when compared to other nuclei. Within the thalamus, the spatial distribution showed a gradual increase from the tail to the head. In contrast to the other three transmitter/transporters, M1, a receptor categorized as a muscarinic acetylcholine transmitter system, showed high concentrations in the nucleus accumbens, putamen, and caudate head, with moderate concentrations in the amygdala and hippocampus, but with lowest expression in the thalamus.

2.4 Associations between morphological alteration levels and neurotransmitter profiles

We used the MSA to parcellate the vertex-wise *t*-statistics of both JD and RD. We then extracted parcel-wise *t*-statistics (Suppl. Figure 2) and associated them with parcellated neurotransmitter profiles (Fig. 3B). The deviation level of the shape area of the GGE group was associated with expression of the acetylcholine (ACh) and NE transmitter systems. The shape area deviation was strongly correlated with expression of the nicotinic ACh receptor, $\alpha_4\beta_2$ (r_s = 0.60, p_{SAC} = 0.01, SAC, spatial autocorrelation corrected), but negatively correlated to the muscarinic ACh receptor, M_1 (r_s = -0.53, p_{SAC} = 0.045). The shape area deviation map also correlated to NET expression (source1: r_s = 0.52, p_{SAC} = 0.04; source 2: r_s = 0.60, p_{SAC} = 0.02). No significant correlation was found between the shape area deviation profile and other neurotransmitter maps (Suppl. Table 2), and no significant result was found between the shape thickness deviation profile and all neurotransmitter maps (Suppl. Table 2).

3. Discussion

We systematically characterized shape alterations of 14 subcortical structures in GGE using a surface-based morphological analysis pipeline. We found that GGE was associated with extensive morphological changes in the shape of all subcortical structures. Using a collective toolbox that aggregated neurotransmitter profiles derived from PET scans, we found that shape area deviations were associated with multiple neurotransmitter expression profiles across different systems, including acetylcholine and norepinephrine. These results increased our understanding of the relationship between macroscale morphological information and microscale molecular pathways in GGE.

Subcortical structures play a critical role in behavioral symptoms, propagation, and even initiation of epileptic seizures[33]. However, the pattern and extent of subcortical structural disruptions due to epilepsy development is still unclear, given the absence of systematic examination of fine-grained morphological features. Our study utilized a surface-based pipeline to provide detailed morphometric information on the subcortical nuclei in GGE patients. The morphological profiles examined in this study included distances between each vertex to the medial curve of the specific structure, namely the shape thickness; and the surface dilation ratio of mapping the corresponding vertex on individual surfaces to the standard template, namely the shape area. These two metrics described the fundamental structural property of the subcortical nuclei. Compared to volumetric analysis, the surface-based pipeline provided a more precise representation of the shape of brain structures, and was better able to distinguish morphological abnormalities. While inconsistent results have been reported in previous volumetric analyses, and a systematic examination of subcortical structures remains lacking, our study indicated that GGE patients had widespread morphological alterations in both shape thicknesses and areas. The deviation patterns of shape areas and thicknesses were coarsely symmetric across hemispheres, with some apparent asymmetries in the thalamus and ventral hippocampus. Bilateral ventral, medial, and right dorsal thalamus, and bilateral lateral putamen exhibited notable shape surface dilation, whereas other

structures had spatially scattered patterns with mixed dilation and contraction distributions. Compared to previous studies that used volumetric pipelines, we obtained a more fine-grained analysis of the morphological alterations of subcortical nuclei in GGE. These results provided systematic knowledge about the disruption of these structures and potential targets for new hypotheses of pathological circuits, as well as detailed locations for precision intervention and associations to other modalities.

Neurotransmitters play an increasing role in the theory of pathogenesis of epilepsy, including GGE. The development of new generation anti-epileptic drugs that target the restoration of the balance between neurotransmitters is a core element of this theory, as opposed to mainstream anti-seizure medications, which only provide symptomatic relief[29]. Our results provided a comprehensive characterization of the relationship between subcortical structural vulnerabilities and neurotransmitter profiles. We examined the associations of the disruption levels of both shape areas and thicknesses using PET-derived neurotransmitter expression maps across nine different systems, and found two kinds of neurotransmitter profiles, which provided a close relationship with the shape area deviation pattern of GGE: Ach and NE. Ach is a neurotransmitter that consists of acetic acid and choline ester[34], and is involved in multiple cognitive functions, including memory and learning[35]. Animal and preclinical studies have suggested dysfunction of the cholinergic system, mediated by release of ACh, which may lead to epilepsy[36]. Several studies have reported that ACh and related receptors and precursors were involved in the pathogenesis of epilepsy[37–39]. The profiles of two ACh subtype receptors, muscarinic and nicotinic Ach, exhibited distinct relationships to shape area deviations. The muscarinic ACh (M_1) expression profile of subcortical structures was negatively correlated with shape area alteration levels, which suggested that the effect of GGE exerted in subcortex may involve muscarinic Ach, because low concentration areas were more vulnerable to structural damage. Muscarinic ACh (M_1) has been shown to be involved in the initiation of generalized epileptic seizures in the subcortex of rat models[40], and is also associated with hippocampal dysfunction[41]. In contrast, the nicotinic ACh (α4β2) profile exhibited positive correlations with shape area deviations, suggesting a possible molecular mechanism involving nicotinic Ach, leading to subcortex structural disruptions in GGE. Previous studies have reported that nicotinic ACh receptors, which are extensively expressed in hippocampal neurons, may contribute to epilepsy, with decreased expression being observed in patients[42]. In the present study, we found a significant correlation between NET expressions and shape area deviations in two PET maps from different sources. NE is produced from dopamine and released from noradrenergic neurons as a neurotransmitter[43]. NE is deemed as a seizure suppressor[44] and may also play a part in seizure modulation by slowing the stimulation of limbic areas[29].

The present study showed widespread structural alterations of subcortical nuclei in GGE. The surface-based subcortical morphological pipeline was more effective at detecting fine-grained defects than its volumetric counterparts. The results indicated a general abnormality of shape morphology in all subcortical structures included in the analysis, with the most significant disruptions found in the thalamus, putamen, and hippocampus. Volumetric PET data, which analyzed neurotransmitter profiles,

was transformed to shape surfaces and associated with morphological deviation patterns. Two types of neurotransmitters, ACh and NE, were shown to be closely related to morphological disruptions. Taken together, these results provided a comprehensive characterization of subcortical morphological disruptions, and suggested corresponding molecular pathways that may aid the development of new types of anti-epileptic drugs and precision interventions, as well as expand our understanding of the pathogenesis of GGE.

4. Methods

4.1 Participants

We retrospectively enrolled a cohort of patients with a diagnosis of GGE. All patients underwent a structural brain scan between April 2007 and October 2016 at Jinling Hospital, Nanjing, China. This retrospective study was approved by the local medical ethics committee at Jinling Hospital, Nanjing University School of Medicine, China. Written informed consent was obtained from all participants.

Two experienced neurologists performed the diagnoses according to the following criteria. Seizure symptoms involved patients presenting with typical seizure semiology of generalized tonic-clonic seizures (GTCS), including loss of consciousness during seizures without precursory symptoms of partial epilepsy or aura, and tonic extensions of the limbs followed by a clonic phase of rhythmic jerking. Scalp electroencephalogram (EEG) involved generalized spike-and-wave discharges on EEG. No other epilepsy-associated etiology existed; patients had no other history of epilepsy-associated etiology, such as trauma, tumor, or intracranial infection. The HCs had no history of neurological disorder or psychiatric illness, and no gross abnormality in brain MRI images. They were sex- and age-matched with the GGE group. All participants recruited in this study were right-handed.

4.2 MRI acquisition

All participants underwent structural magnetic resonance imaging scans with a Siemens Trio 3-Tesla scanner (Siemens, Munich, Germany) at Jinling Hospital, Nanjing, China. Foam padding was used to minimize head motion. Participants were required to keep their eyes closed, their head still, and to avoid falling asleep. High resolution T1-weighted (T1w) images were acquired in the sagittal orientation using a magnetization-prepared rapid gradient-echo sequence (TR = 2,300 ms, TE = 2.98 ms, flip angle = 9°, FOV = 256 × 256 mm^2, matrix size = 256 × 256, slice thickness = 1 mm, no interslice gap, voxel size = 1 × 1 × 1 mm^3, with 176 slices). All patients were in an interictal state throughout the scanning process.

4.3 MRI data processing

T1w structural images were processed using FreeSurfer[45] (version 7.1.1) to acquire structure segmentations and volumetric statistic summaries of the bilateral subcortical structures, including the thalamus, caudate, putamen, pallidum, hippocampus, amygdala, and nucleus accumbens.

We used the ENIGMA-Shape pipeline to conduct the subcortical morphometric analysis. This pipeline has been validated for test-retest reliability. The pipeline includes three main steps: surface reconstruction, registration, and shape metrics computation (Fig. 1). A mesh model was constructed for each individual FreeSurfer-parcellated subcortical region. The mesh was inflated to a spherical mesh and registered to a structure-specific template spherical mesh by matching the local geometric features. After registering individual meshes to the standard template, two surface vertex-wise morphological measures were defined: radial distance (RD) and Jacobian determinant (JD). The RD was the distance of each vertex to the medial curve, which was the core along the long axis of the structural skeleton. The JD was the surface dilation ratio of mapping the corresponding vertices on individual-specific structure surfaces to the standard templates. Because the distribution of the JD tended to be non-Gaussian, logarithm-transformed JD was used to obtain a distribution closer to a Gaussian distribution.

4.4 Neurotransmitter receptor and transporter data

We collected receptor and transporter data across nine neurotransmitter systems from the Neuromaps toolbox[32,46], aggregating positron emission tomography (PET) data from more than 1,200 healthy individuals. All data downloaded from the Neuromaps toolbox were in MNI 152 2 mm cubic space.

4.5 Shape space projection

To associate subcortical shape features with neurotransmitter profiles, we projected the Melbourne Subcortex Atlas[27] (MSA, 3T, Scale IV version, 54 bilateral subcortical regions) to the shape surface (Fig. 3A). Specifically, we used the s2v function from the iso2mesh toolbox to convert the shape surface mesh to a volumetric image, which we called the volumetric shape template. We then linearly registered this volumetric shape template to MNI space using FLIRT[47] (part of FSL) to obtain the transform matrix parameters. We computed the coordination of the center of gravity (CoG) of all subcortical regions in the MSA (MNI 152 space) and projected the CoG coordinates to the volumetric shape template using the aforementioned transform matrix. We then projected the CoG coordinates back to the shape surface space by using the *v2smap* function in iso2mesh toolbox. We followed a winner-takes-all routine to assign each vertex to the nearest CoG of MSA regions in a structure- and hemisphere-specific manner. This resulted in an MSA atlas in shape surface. Neurotransmitter maps were parcellated by the original volumetric MSA atlas and projected to homologous regions in the surface MSA atlas.

4.6 Statistical analysis

All the vertex-level statistical tests were conducted using the *SurfStat* toolbox. The two surface-based subcortical shape metrics were compared between the two groups using a two sample *t*-test, with age, sex, and whole brain volume as covariates. Multiple test corrections were also conducted using *SurfStat*, with the family-wise error (FWE) controlled at $p_{FWE} < 0.05$.

The association between *t*-value maps of shape metrics and neurotransmitter maps was quantified by computing Spearman's correlation coefficient. The statistical significance of the correlation coefficient

was determined by its percentile rank compared to a spatial autocorrelation permutation null (5,000 times), which was constructed using the *BrainSMASH* toolbox.

4.7 Data and code availability

The supporting data of the figures, tables and customized code will be available on GitHub at https://github.com/YaoMeng94/GGE_Shape.

Declarations

Acknowledgement

The authors would like to express their sincere gratitude to all participants who participated in this study.

Funding

This work is supported by the National Key Project of Research and Development of Ministry of Science and Technology (2022YFC2009900 and 2022YFC2009906); National Natural Science Foundation of China (82202250, 62276051, 62036003, 61876156, 82302293) and the Fundamental Research Funds for the Central Universities (ZYGX2022YGRH008).

Competing interests

The authors declare no known competing interests.

References

1. Royer, J. *et al.* Cortical microstructural gradients capture memory network reorganization in temporal lobe epilepsy. 2022.10.31.513891 Preprint at https://doi.org/10.1101/2022.10.31.513891 (2022).
2. Jallon, P. & Latour, P. Epidemiology of Idiopathic Generalized Epilepsies. *Epilepsia* **46**, 10–14 (2005).
3. Woermann, F. G., Sisodiya, S. M., Free, S. L. & Duncan, J. S. Quantitative MRI in patients with idiopathic generalized epilepsy. Evidence of widespread cerebral structural changes. *Brain* **121**, 1661–1667 (1998).
4. Bernhardt, B. C. *et al.* Thalamo–cortical network pathology in idiopathic generalized epilepsy: Insights from MRI-based morphometric correlation analysis. *NeuroImage* **46**, 373–381 (2009).
5. Liao, W. *et al.* Altered relationship between thickness and intrinsic activity amplitude in generalized tonic–clonic seizures. *Sci. Bull.* **61**, 1865–1875 (2016).
6. Bernasconi, A. *et al.* Magnetic resonance spectroscopy and imaging of the thalamus in idiopathic generalized epilepsy. *Brain* **126**, 2447–2454 (2003).

7. Natsume, J., Bernasconi, N., Andermann, F. & Bernasconi, A. MRI volumetry of the thalamus in temporal, extratemporal, and idiopathic generalized epilepsy. *Neurology* **60**, 1296–1300 (2003).
8. Du, H. *et al.* Regional atrophy of the basal ganglia and thalamus in idiopathic generalized epilepsy. *J Magn Reson Imaging* **33**, 817–821 (2011).
9. Park, K. M., Kim, S. E., Lee, B. I. & Hur, Y. J. Brain Morphology in Patients with Genetic Generalized Epilepsy: Its Heterogeneity among Subsyndromes. *European Neurology* **80**, 236–244 (2019).
10. Betting, L. E. *et al.* MRI volumetry shows increased anterior thalamic volumes in patients with absence seizures. *Epilepsy & Behavior* **8**, 575–580 (2006).
11. Li, X. *et al.* Atrophy in the Left Amygdala Predicted Drug Responses in Idiopathic Generalized Epilepsy Patients With Tonic–Clonic Seizures. *Frontiers in Neuroscience* **15**, (2021).
12. Chan, C. H. (Patrick) *et al.* Thalamic Atrophy in Childhood Absence Epilepsy. *Epilepsia* **47**, 399–405 (2006).
13. Roshchupkin, G. V. *et al.* Heritability of the shape of subcortical brain structures in the general population. *Nat Commun* **7**, 13738 (2016).
14. Gutman, B. A. *et al.* A Riemannian Framework for Intrinsic Comparison of Closed Genus-Zero Shapes. in *Information Processing in Medical Imaging* (eds. Ourselin, S., Alexander, D. C., Westin, C.-F. & Cardoso, M. J.) 205–218 (Springer International Publishing, 2015). doi:10.1007/978-3-319-19992-4_16.
15. Gutman, B. A. *et al.* Medial demons registration localizes the degree of genetic influence over subcortical shape variability: An N= 1480 meta-analysis. in *2015 IEEE 12th International Symposium on Biomedical Imaging (ISBI)* 1402–1406 (2015). doi:10.1109/ISBI.2015.7164138.
16. Gutman, B. A. *et al.* Maximizing power to track Alzheimer's disease and MCI progression by LDA-based weighting of longitudinal ventricular surface features. *NeuroImage* **70**, 386–401 (2013).
17. Gutman, B. A., Madsen, S. K., Toga, A. W. & Thompson, P. M. A Family of Fast Spherical Registration Algorithms for Cortical Shapes. in *Multimodal Brain Image Analysis* (eds. Shen, L. et al.) 246–257 (Springer International Publishing, 2013). doi:10.1007/978-3-319-02126-3_24.
18. Gutman, B. A., Wang, Y., Rajagopalan, P., Toga, A. W. & Thompson, P. M. Shape matching with medial curves and 1-D group-wise registration. in *2012 9th IEEE International Symposium on Biomedical Imaging (ISBI)* 716–719 (2012). doi:10.1109/ISBI.2012.6235648.
19. Gutman, B., Wang, Y., Morra, J., Toga, A. W. & Thompson, P. M. Disease classification with hippocampal shape invariants. *Hippocampus* **19**, 572–578 (2009).
20. Ching, C. R. K. *et al.* Sex-Dependent Age Trajectories of Subcortical Brain Structures: Analysis of Large-Scale Percentile Models and Shape Morphometry. 2020.09.30.321711 Preprint at https://doi.org/10.1101/2020.09.30.321711 (2020).
21. Li, B. *et al.* Influence of APOE Genotype on Hippocampal Atrophy over Time - An N=1925 Surface-Based ADNI Study. *PLoS One* **11**, e0152901 (2016).

22. Wang, Y. *et al.* Surface-based TBM boosts power to detect disease effects on the brain: an N=804 ADNI study. *Neuroimage* **56**, 1993–2010 (2011).
23. Roussotte, F. F. *et al.* Apolipoprotein E epsilon 4 allele is associated with ventricular expansion rate and surface morphology in dementia and normal aging. *Neurobiol Aging* **35**, 1309–1317 (2014).
24. Wade, B. S. C. *et al.* Effect of Electroconvulsive Therapy on Striatal Morphometry in Major Depressive Disorder. *Neuropsychopharmacology* **41**, 2481–2491 (2016).
25. Ho, T. C. *et al.* Subcortical shape alterations in major depressive disorder: Findings from the ENIGMA major depressive disorder working group. *Hum Brain Mapp* **43**, 341–351 (2022).
26. Gutman, B. A. *et al.* A meta-analysis of deep brain structural shape and asymmetry abnormalities in 2,833 individuals with schizophrenia compared with 3,929 healthy volunteers via the ENIGMA Consortium. *Hum Brain Mapp* hbm.25625 (2021) doi:10.1002/hbm.25625.
27. Tian, Y., Margulies, D. S., Breakspear, M. & Zalesky, A. Topographic organization of the human subcortex unveiled with functional connectivity gradients. *Nat Neurosci* **23**, 1421–1432 (2020).
28. Ching, C. R. K. *et al.* Mapping Subcortical Brain Alterations in 22q11.2 Deletion Syndrome: Effects of Deletion Size and Convergence With Idiopathic Neuropsychiatric Illness. *AJP* **177**, 589–600 (2020).
29. Akyuz, E. *et al.* Revisiting the role of neurotransmitters in epilepsy: An updated review. *Life Sciences* **265**, 118826 (2021).
30. Werner, F.-M. & Covenas, R. Classical Neurotransmitters and Neuropeptides Involved in Generalized Epilepsy: A Focus on Antiepileptic Drugs. *CMC* **18**, 4933–4948 (2011).
31. Blumenfeld, H. From Molecules to Networks: Cortical/Subcortical Interactions in the Pathophysiology of Idiopathic Generalized Epilepsy. *Epilepsia* **44**, 7–15 (2003).
32. Hansen, J. Y. *et al.* Mapping neurotransmitter systems to the structural and functional organization of the human neocortex. *Nat Neurosci* (2022) doi:10.1038/s41593-022-01186-3.
33. Norden, A. D. & Blumenfeld, H. The role of subcortical structures in human epilepsy. *Epilepsy & Behavior* **3**, 219–231 (2002).
34. Sam, C. & Bordoni, B. Physiology, Acetylcholine. (2023).
35. Gigout, S. *et al.* Muscarinic acetylcholine receptor-mediated effects in slices from human epileptogenic cortex. *Neuroscience* **223**, 399–411 (2012).
36. Gigout, S., Wierschke, S., Dehnicke, C. & Deisz, R. A. Different pharmacology of N-desmethylclozapine at human and rat M2 and M4 mAChRs in neocortex. *Naunyn-Schmiedeberg's Arch Pharmacol* **388**, 487–496 (2015).
37. Lee, M., Young Choi, B. & Won Suh, S. Unexpected Effects of Acetylcholine Precursors on Pilocarpine Seizure- Induced Neuronal Death. *Current Neuropharmacology* **16**, 51–58 (2018).
38. Hillert, M. H. *et al.* Dynamics of hippocampal acetylcholine release during lithium-pilocarpine-induced status epilepticus in rats. *Journal of Neurochemistry* **131**, 42–52 (2014).
39. Iha, H. A. *et al.* Nicotine Elicits Convulsive Seizures by Activating Amygdalar Neurons. *Frontiers in Pharmacology* **8**, (2017).

40. Cruickshank, J. W., Brudzynski, S. M. & McLachlan, R. S. Involvement of M1 muscarinic receptors in the initiation of cholinergically induced epileptic seizures in the rat brain. *Brain Research* **643**, 125–129 (1994).
41. Broncel, A., Bocian, R., Kłos-Wojtczak, P. & Konopacki, J. Medial septal cholinergic mediation of hippocampal theta rhythm induced by vagal nerve stimulation. *PLoS ONE* **13**, e0206532 (2018).
42. Baranowska, U. & Wiśniewska, R. J. The α7-nACh nicotinic receptor and its role in memory and selected diseases of the central nervous system. *Postepy Hig Med Dosw (Online)* **71**, 633–648 (2017).
43. Goldstein, D. S. Adrenaline and Noradrenaline. in *Encyclopedia of Life Sciences* (John Wiley & Sons, Ltd, 2010). doi:10.1002/9780470015902.a0001401.pub2.
44. Hui Yin, Y., Ahmad, N. & Makmor-Bakry, M. Pathogenesis of epilepsy: challenges in animal models. *Iran J Basic Med Sci* **16**, 1119–1132 (2013).
45. Fischl, B. FreeSurfer. *NeuroImage* **62**, 774–781 (2012).
46. Markello, R. D. *et al.* neuromaps: structural and functional interpretation of brain maps. *Nat Methods* 1–8 (2022) doi:10.1038/s41592-022-01625-w.
47. Jenkinson, M., Beckmann, C. F., Behrens, T. E. J., Woolrich, M. W. & Smith, S. M. FSL. *NeuroImage* **62**, 782–790 (2012).

Figures

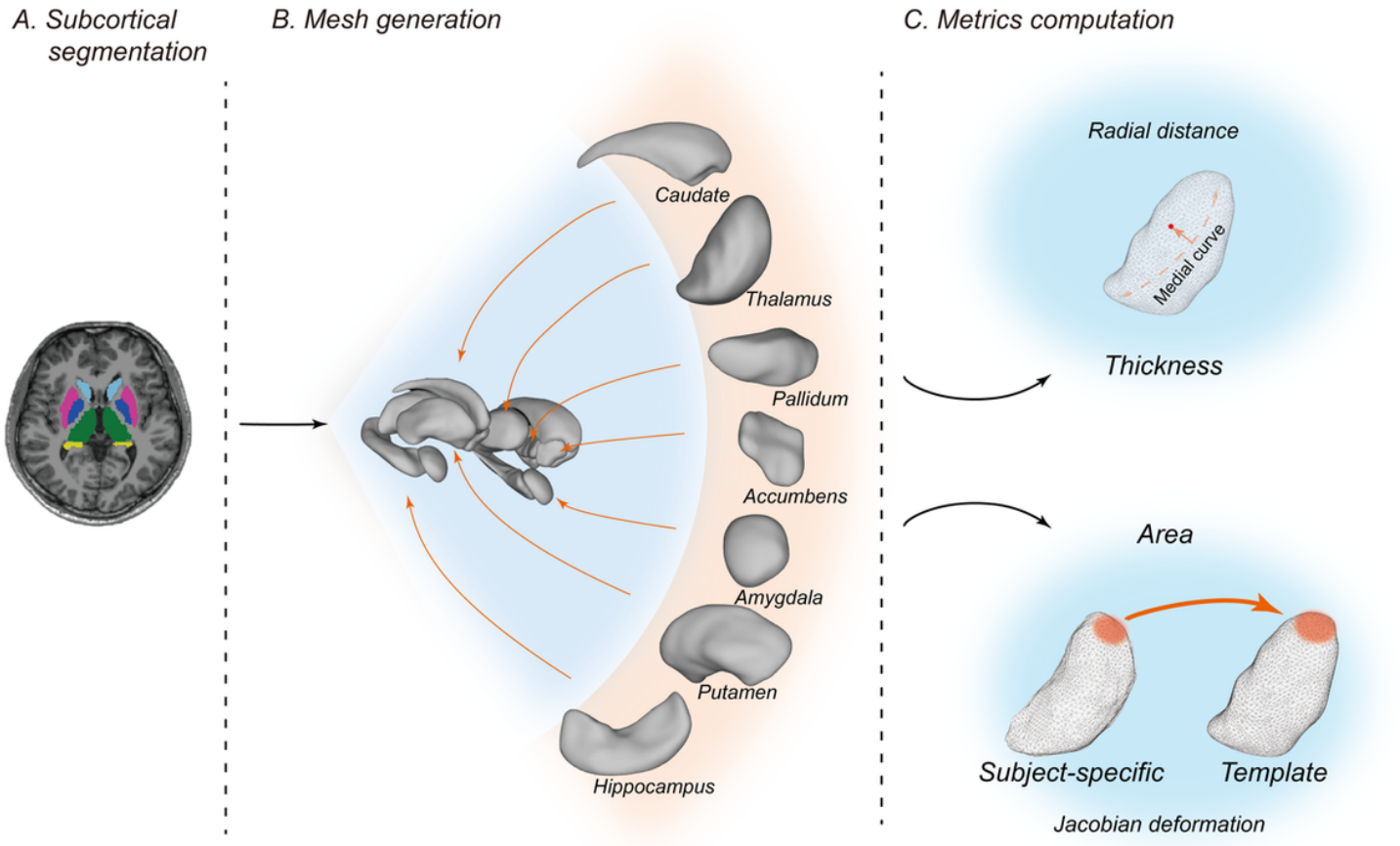

Figure 1

Schematic of the ENIGMA Shape pipeline. (A) Seven bilateral subcortical structures were defined based on individualized FreeSurfer segmentation (aseg). (B) Mesh models were constructed for the caudate, thalamus, pallidum, accumbens, amygdala, putamen, and hippocampus. (C) Two vertex-wise morphological measures were defined: radial distance, which is the core along the long axis of the structural skeleton and empirically considered to be a measure of shape “thickness”, and Jacobian determinant, defined as the surface dilation ratio of mapping the corresponding vertices on individual-specific structure surfaces to the standard template, and considered to be a measure of shape “area”.

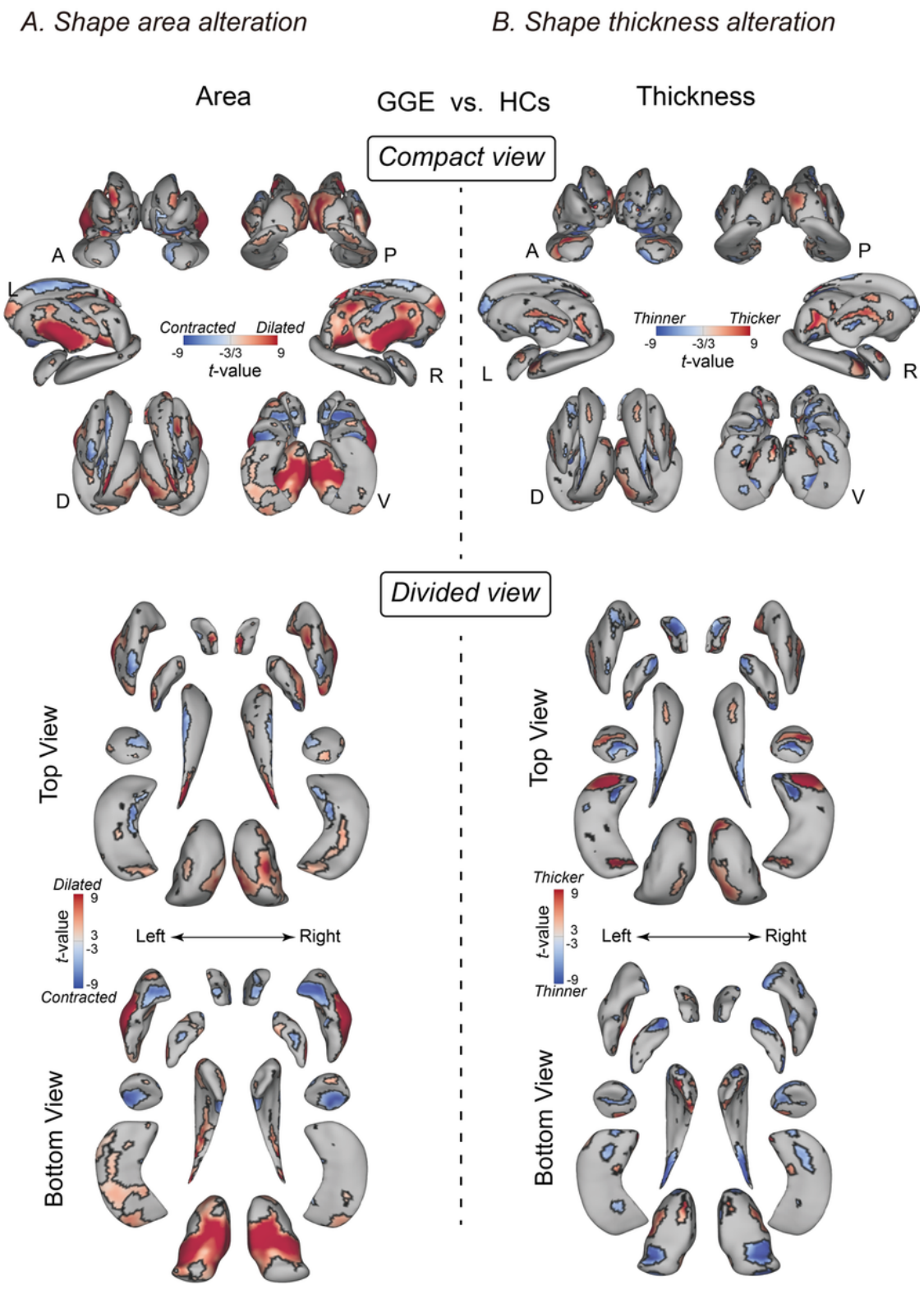

Figure 2

Subcortical shape alterations between genetic generalized epilepsies (GGE) and healthy controls (HCs). Statistical differences between GGE and HCs involving shape areas (A) and thicknesses (B) were rendered on the shape mesh. Surface-wide statistical comparisons were conducted using a two-sample *t*-test, with all cluster family-wise error controlled at $p_{FWE} < 0.05$. The *t*-value maps are rendered on the

actual shape mesh in the compact view and the split shape mesh in the divided view. The abbreviations A, P, L, R, D, and V refer to anterior, posterior, left, right, dorsal, and ventral views, respectively.

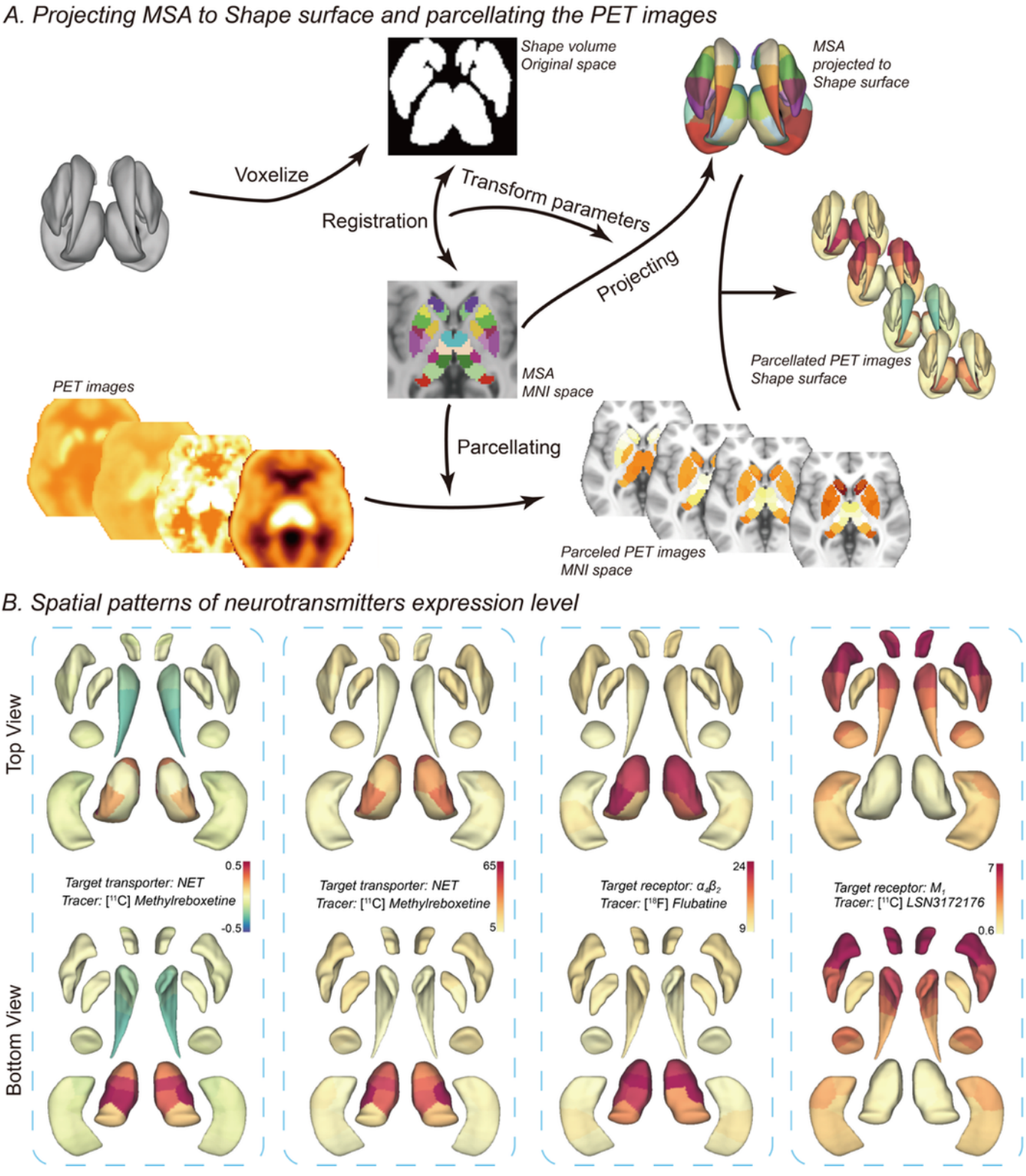

Figure 3

Projection of the Multiple Scale Atlas (MSA) and neurotransmitter profiles on the shape mesh. (A) Demonstration of the projection of the MSA from MNI volumetric space to shape mesh. (B) Selected

neurotransmitter/transporter profiles are rendered on the split shape mesh. The left two maps show the expression of norepinephrine transporter from two different sources. The middle and right maps show the $\alpha_4\beta_2$ and M_1 receptors, respectively.

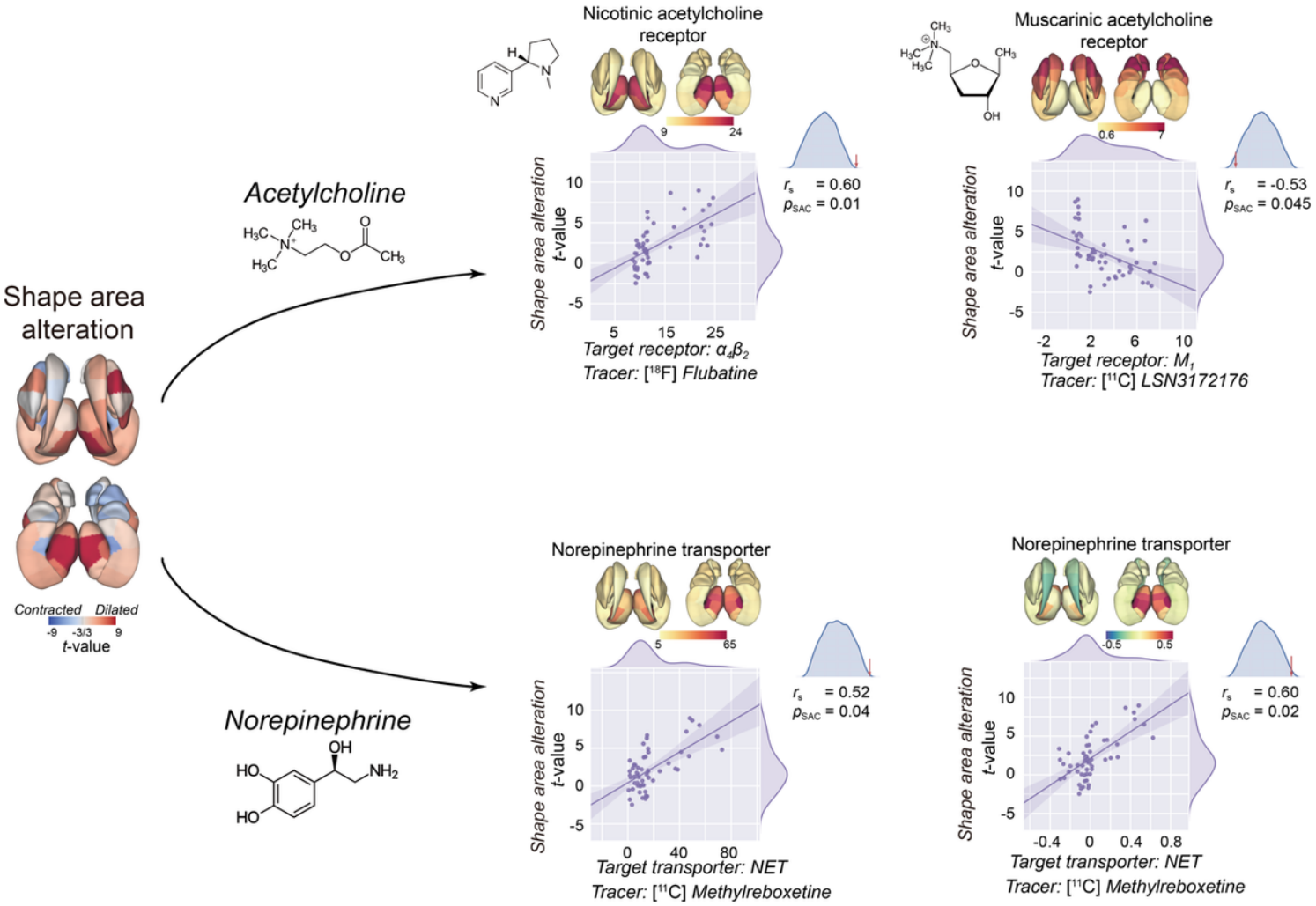

Figure 4

Associations between surface-based subcortical shape alteration levels and neurotransmitter profiles. Correlations between parcellated shape area *t*-maps and parcellated neurotransmitter profiles. r_S: Spearman's correlation coefficient; p_{SAC}: spatial autocorrelation corrected p-value.

Supplementary Files

This is a list of supplementary files associated with this preprint. Click to download.

- GTCSshapeV6SI.docx